The University of California
Space Sciences Laboratory

and

Lawrence Berkeley Laboratory
Berkeley, California 94720

Semi-Annual Report

HEAVY ION FRAGMENTATION EXPERIMENTS AT THE BEVATRON

NASA Grant NGR 05-003-513

Principal Investigator
Dr. Harry H. Heckman

Period Covered
1 April 1975 to 30 September 1975

November 17, 1975

Space Sciences Laboratory Series 16, Issue 69

ABSTRACT

This report describes the continued collaborative research effort between the University of California Space Sciences Laboratory and the Lawrence Berkeley Laboratory to study the fragmentation processes of heavy nuclei in matter using the recently developed heavy-ion capability of the Bevatron. The purpose of the research program is to obtain the single particle inclusive spectra of secondary nuclei produced at 0^{o} by the fragmentation of heavy ion beam projectiles. The process being examined is B+T → F + anything, where B is the beam nucleus, T is the target nucleus, and F is the detected fragment. The fragments F are isotopically identified by experimental procedures involving magnetic analysis, energy loss and time-of-flight measurements. In progress are measurements of the partial differential cross-sections for all nuclides (p, ^{4}He, ^{10}Be, ..., etc) produced at 0 ± 12.5 mrad by the fragmentation of beam particles ^{12}C, ^{14}N, ^{15}N, ^{16}O and ^{40}Ar as a function of energy $1.05 \leq E \leq 2.1$ GeV/nucleon and mass number A of target nucleus.

The principal objectives of the experiment are: a) to study the fragmentation processes of heavy nuclei in matter, b) to measure the total and partial production cross section for all isotopes, c) to test the applicability of high-energy multi-particle interaction theory to nuclear fragmentation, d) to apply the cross-section data and fragmentation probabilities to cosmic ray transport theory and e) to search for systematic behavior of fragment production as a means to improve existing semi-empirical theories of cross-sections.

An important activity derived from this research is the use of a 0-degree magnetic spectrometer by experimenters for the purposes of calibrating cosmic-ray detectors. To support such experiments, we are presently augmenting the capability of this system to perform for user groups on-line graphics, data collection and diagnostics using a (GT-40) Graphic Terminal combined with linked PDP 11/45 and 11/20 computers.

HEAVY ION FRAGMENTATION EXPERIMENTS AT HIGH ENERGY

I. INTRODUCTION

This report describes our efforts during the period 1 October 1974 to 30 October 1975, under NASA Grant NGR 05-003-513, in the research program to study the nuclear interactions of relativistic heavy nuclei in the laboratory. This program is being performed at the Bevalac, and is a collaborative effort between the University of California Space Sciences Laboratory and the Lawrence Berkeley Laboratory. The unique capability of the Bevalac to accelerate heavy ions to energies up to 2.6 GeV/nucleon affords us the single opportunity to explore a new field of research which is becoming increasingly important to cosmic ray physics, high energy particle physics and nuclear physics. A fundamental problem of cosmic rays is the establishment of the age and source composition of the galactic cosmic rays. The heavy ion component of this radiation offers one of the best clues for the understanding of this question--provided the pertinent fragmentation cross sections for interaction with interstellar matter are known. The principal objective of this research is to measure these fragmentation cross sections for beam nuclei, beginning with ^{4}He, ^{12}C, ^{14}N, and ^{16}O, $1.05 \leq E \leq 2.1$ GeV/nucleon,in various targets H through Pb.

The method of the experiment is to obtain the single particle inclusive spectra of secondary nuclei produced at 0^{o} by the fragmentation of heavy ion beam projectiles. The process being examined is B+T→F+ ----, where B is the beam nucleus, T is the target nucleus, and F is the detected fragment. The fragments F are isotopically identified by experimental procedures involving magnetic analysis, energy loss and time-of-flight measurements. Currently being measured are the partial differential cross-sections for all nuclides (p, ^{4}He, ^{10}Be,...., etc.) produced at 0 ± 12.5 mrad by the fragmentation of beam particles ^{12}C, ^{14}N, ^{15}N, ^{16}O and ^{40}Ar as a function of energy and mass number A of target nucleus.

II. PURPOSES AND OBJECTIVES OF THE RESEARCH PROGRAM

The specific purpose of the program is to carry out experiments on the single-particle inclusive spectra of the nuclei produced at 0^{o} by the fragmentation of high energy, heavy-ion beam projectiles. The process we are considering is B+T→F+ anything, where B is the beam (projectile) nucleus, T is the target nucleus, and F is the detected fragment. The purposes of the experiment in progress are:

1) To measure the total inelastic cross sections for primary particles, such as ^{12}C, ^{14}N and ^{16}O, as a function of energy, $1.05 \leq E \leq 2.1$ GeV/nucleon, and mass number A of the target nucleus. In addition, similar measurements may be done using isotopically identified secondary beams of stable and radioactive fragmentation products of the primary beam. Such nuclei will include isotopes of Li, Be, B and C. Target materials will range from hydrogen (A=1) to Pb (A=207).

2) To measure the partial differential cross sections for the production of all nuclides (p, ^{4}He, ^{10}Be, ^{11}C, ..., etc.) produced at $\pm$ 12.5 mrad. by the fragmentation of primary beam particles and their dependences of energy and target nucleus.

The objectives of the experimental program are:

1) To test experimentally the concepts of limiting fragmentation and the factorization of cross-sections when applied to hadron-hadron systems with large baryon numbers; namely, that the fragmentation cross sections attain asymptotic (constant) values at high energies, and the modes of fragmentation are independent of the target-nucleus.

2) To determine the transverse and longitudinal momentum distributions that are characteristic of the fragmentation process (e.g., internal motion, final state interactions, etc.,) for each isotope F (A,Z) produced in the fragmentation of beam projectile B (A,Z).

3) To search for the possible existence of "proton-rich" light nuclei, such as ^{11}N, ^{8}C, etc., that may be produced in fragmentation of beam nuclei.

4) To search for systematic behavior of fragment production as a means to improve existing semi-empirical theories of cross-sections.

5) To apply the cross section data and fragmentation probabilities of the light and medium nuclei to the problem of the transformation of cosmic ray nuclei by collisions with interstellar hydrogen and helium nuclei.

6) To compare and interpret the observed fragmentation modes of nuclei with nuclear cascade theory.

III. SCIENTIFIC ASPECTS

A. Status of Investigation

Our current experiments on the fragmentation of ^{12}C and ^{16}O nuclei[1,2,3], see Appendices I and II, continue and extend earlier work on the 0^o - fragmentation of ^{14}N beam nuclei at 2.1 GeV/nuclei.[4,5] Figure 1 is a scale drawing of the 0^o heavy-ion magnetic spectrometer, taken from ref. 6, that has been designed and brought into operation to carry out the 0-deg fragmentation experiments. The spectrometer focuses magnetically analysed beam fragments, produced within 12.5 mr of the beam direction, onto charge-measuring solid-state detector telescopes placed along the focal plane of the spectrometer. A detailed description of the spectrometer facility and its applicability to calibration experiments is given in Ref. 6

During the first 24 months of this work, experimental data on the fragmentation of ^{12}C, ^{14}N, ^{15}N, ^{16}O and ^{40}Ar beams at 2.1 GeV/n and ^{12}C at 1.05 GeV/n have been collected. We have recently completed the analysis of the ^{12}C and ^{16}O data. The highlights of our results are outlined below. Refer to Appendices I and II for more detailed statements on this work.

Summary of Results.

i) within the momentum range allowed by our magnetic spectrometer, the fragmentation of high-energy beam projectiles produces all known isotopes having mass numbers A equal to, or less than, that of the projectile. Figure 2 illustrates the observed spectra of the carbon isotopes produced by the fragmentation of ^{16}O at 2.1 GeV/nucleon.

ii) the longitudinal momentum distributions of the nuclear fragments in the rest frame of the (moving) projectile are Gaussian shaped, with S. D. widths 50 to 200 MeV/c. The widths are dependent on the projectile and fragment, but independent of target mass (H through Pb) and beam energy. (Appendix I)

iii) 464 partial-production cross sections for 35 isotopes have been measured -- a 20 fold increase in the known heavy-ion fragmentation cross sections data above 1 GeV/n. (Appendix II).

iv) The cross sections are energy independent and are factorable into beam (B)-fragment (F) and target (T) terms, e.g., $\sigma_{BT}^{F}=\gamma_{B}^{F}\,\gamma_{T}$, where σ_{BT}^{F} is the cross section for the reaction B+T → F + = --. The quantity γ_T is the target factor. To an accuracy of about 10%, $\sigma_{BT}^{F} = \sigma_{BH}^{F}\,A_T^{1/4}$, i.e., the cross section for the production of the fragment F is the product of the cross section for the production of the fragment F in hydrogen and $A_T^{1/4}$, where A_T is the mass number of the target nucleus. (Appendix II).

v) An exception of strict factorization occurs for single-nucleon stripping in high-Z targets. These cross sections include a component for Coulomb dissociation, via the giant dipole resonance, in the target's virtual photon field. This is the first observation of this effect.

B. Applications to Cosmic Ray Physics

The field of cosmic ray physics stands to benefit most immediately from heavy ion research. Dramatic advances in our knowledge of the elemental and isotopic composition of the cosmic rays in the interstellar medium have been made from recent balloon and satellite experiments, and theoretical-computational techniques to interpret these observations in terms of transport equations are available. However, the gross lack of interaction and fragmentation cross sections of cosmic ray nuclei with the interstellar gas necessary for solving the transport problem precludes and understanding of the primordial composition of the cosmic rays. It is, in fact, the lack of comprehensive laboratory data on the fragmentation cross sections that has become a principal impediment to progress in this area of cosmic-ray research.

Experiments with high energy proton beams do not simulate well the fragmentation process as it occurs in space. In particular, realistic proton targets are thick compared with the ranges of most secondary fragments. With the heavy ion capability of the Bevatron, the fragmentation of cosmic-ray nuclei can be observed "in situ".

Although the heavy nuclei in the primary cosmic rays comprise less than 1% of the total cosmic ray flux, they contain much information on the interstellar medium, the regions of cosmic-ray confinement, and motions of magnetic field lines in the galaxy. Clues to the sources of the cosmic rays and the nature of the of the primordial radiation at the sources are being obtained from studies of the compositions and energy spectra of arriving heavy nuclei. Too, in the near future, information on the isotopic composition will be forthcoming. The interpretation of these observations, given the relevant fragmentation cross-sections of the heavy ions in the H and He interstellar gas, will have an impact on many areas of astrophysics. Comprehensive information on the nuclear transformation on the nuclear transformation of the primary cosmic rays can give us detailed insights on the interstellar medium, and on the confinement and leakage of cosmic rays from the galaxy. Knowledge of the cross sections for the nuclear transformations of cosmic ray nuclei thus leads to information on the primordial composition itself, while imposing constraints on source models. To retrieve this abundance of astrophysical information requires accurate fragmentation cross sections. The experimental results outlined above is a strong testament that our current project can, and shall, yield this cross section information.

C. NASA Related Research at the Bevalac

An important application of the spectrometer facility used for our fragmentation experiments is the development and calibration of cosmic-ray detectors. Because the heavy-ion spectrometer makes available beams of any isotope of mass less than the incident beam (provided it is particle stable), its use by NASA experimenters has greatly enhanced the value of the facility. To estimate future use of the Bevalac and spectrometer by NASA personnel, the Bevalac Users Association polled potential users of heavy-ion beams among the cosmic-ray community. A total of 13 responses from experimenters whose projects were partially or totally funded by NASA were received. Estimates for heavy-ion beam time given by the NASA projects were: FY '76, 646 hrs, and FY '77, 602 hrs. To assess these estimates, we tabulate the actual use of the heavy-ion spectrometer by NASA projects during the past two years. Listed are the experiment number, investigator, institution and beam time used.

Experiment No.	Investigator	Institution	Beam Time(hrs)
H23	Price	UC Berkeley	151
227 H	Price	UC Berkeley	26
H 30	Price	UC Berkeley	88
H 37	Teegarden	NASA Goddard	15
H 38	Rio	Etude. Nuc. de Saclay	205
H 41	Cartwright	UC Berkeley	21
164 H	Huggett	Louisiana State Univ.	10
165 H	Verma	Louisiana State Univ.	35
H 25	Stone	Cal. Tech.	35
H 16	Greiner	SSL-LBL	31
H 26	Koch	Etude. Nuc. de Saclay	89
H 27	Smith	UC-SSL	58
		Total	764 hrs.

Beam time already requested for calibration runs for calendar dates later then March 1975 are listed below.

Experiment No.	Investigator	Institution	Beam time Requested (hrs)
H 32	Simpson	Univ. of Chicago	80
H 39	Arens	NASA Goddard	--
H 41	Cartwright	UC Berkeley	--
202 H	Verma	Louisiana State Univ.	87
246 H	Waddington	Univ. of Minnesota	96
261 H	Price	UC Berkeley	--
	Stone	Cal. Tech.	48
	Von Rosenvinge	NASA Goddard	72
	Webber	Univ. of Hampshire	16
		Total:	399(+)

IV. TECHNICAL ASPECTS OF RESEARCH PROGRAM

A. Primary Beams

The primary heavy ion beams for these experiments are extracted from the Bevalac and transported in Channel 2 of the External Particle Beam (EPB) and brought to focus at F2 (see Fig. 3). Typical beam parameters required for this proposal are:

Ion	^{4}He	^{12}C	^{14}N	^{16}O
Intensity (max): (particles per pulse on target)	2×10^{10}	1×10^{8}	1×10^{7}	1.5×10^{7}

Intensity (min): 10^{2}/pulse

Energy range: 1.05 to 2.1 GeV/nucleon

Focus: At F2, beam size $\leq$ 1 cm diameter

Emittance: Horizontal = 50 mm mrad, vertical = 100 mm rad.

Pulse: Spill duration of 1 second with a 4 to 6 second period.

B. Magnetic Spectrometer

Figure 3 is a plan view of the magnetic-spectrometer beam system that is being used for a 0^{o} fragmentation experiments. In its present configuration, focal point F2 of the EPB is the source point, and target location, of the spectrometer. Particles emitted within a cone 0 ± 12.5 mrad to the beam are brought to focus at F3, approximately 20 meters from F2. The spectrometer consists of two 8 in. -diameter quadrupole doublets and two bending magnets, M1-M2, and a large sector-shaped vacuum tank between the M2 and F3. The fields of the bending magnets are held constant and the position of the solid-state-telescope detectors defines the particles' rigidity $R = M\beta\gamma/z$ (GV/c). The quadrupole currents are adjusted to bring the desired rigidity into proper focus at F3. The maximum rigidity of particles that can be focussed at F3 by the system is 9 GeV/c.

The rigidity spectra of the fragmentation products transmitted by the spectrometer are obtained by measuring the intensities of the secondaries as a function of distance from the 0^{o} (undeflected) beam line. Particle detectors are mounted on motorized carts whose positions along a curved guide-rail at F3 are controlled and monitored via computer. The maximum excursion is 400 cm from the 0^{o} beam-line.

The characteristics of the spectrometer system are tabulated below.

Rigidity interval:	0 to 9 GV/c (max)
Rigidity resolution:	$\frac{\Delta R}{R} = 0.04 - 0.010$, FWHM
Acceptance angle:	12.5 mrad (max) (Depends on position of F2).

C. Targets

The location of the primary target is F2. A variety of target materials are used in the experiment, including CH_2 (i.e., hydrogen), Be, C, Al, Cu and Pb. Target thicknesses are selected to produce equal changes in the beam rigidity, typically $\Delta R/R \gtrsim 1\text{-}2\%$, in order to sustain an invariant geometry. Later in the program, liquid hydrogen and helium targets will be used.

D. Detection Equipment

1. Particle Identifier: dE/dx Measurements

The heavy ion particle identifiers used in the fragmentation experiments are the result of a program begun at U. C Space Sciences Laboratory in 1967 to optimize the energy-loss information obtainable from solid state detectors for purposes of particle identification [7]. The method is based upon an extensive theoretical foundation,[8] and employs both on-line and off-line computers for acquisition and analysis of the energy-loss data. In the present application, 24 lithium-drifted silicon detectors (2.5 cm in diameter x 3 mm thick) are arranged in six independent groups. each containing four detectors, configured as a telescope. These telescopes can be placed side by side or end to end do achieve a variety of area vs. stopping power arrangements. Each detector has a charge sensitive preamplifier (inside the telescope housing) and a 4095 pulse height analyser.

To analyse the data, the LBL CDC 7600 computer is used to perform a maximum likelihood or χ^2 fit. For each analysed event yielding a set of pulse heights P_1 ---- P_n, the expression $\sum_i^n (P_i-\bar{P})^2/\sigma_i^2$ is minimized with respect to energy, charge, and (in the case of stopping particles) mass. To date, a charge resolution of $\pm$ 0.12e for relativistic heavy

ions and a mass resolution of ±0.1 AMU for stopping ^{16}O and ^{15}O have been achieved. Errors of ±0.1 charge and mass units provide particle identification with confidence levels the order of $1:10^4$.

2. Multiwire Proportional Chambers

A pair of three-plane digitized multiwire proportional chambers are placed behind the solid state detector telescopes. With a spatial resolution of ±0.5 mm and a separation of 1 M between chambers, the trajectory (phase space) of a particle which traverses a telescope can be measured to ±0.5 mm , ±0.5 mrad. Such information maximizes the rigidity resolution of the system and yields differential cross-section data and transverse momentum distributions of the fragments for $P_\perp \lesssim$ 30 MeV/nucleon.

3. Scintillation Counters

Plastic scintillators coupled to photomultiplier tubes are employed at F2 and F3 to 1) monitor primary flux and time structure and 2) provide beam definition and coincidence timing signals and 3) provide time of flight measurements on all analysed fragments with an accuracy of Δt = 150 pico seconds FWHM. For a TOF = 70 nsec, this timing error introduces a fractional mass error $\Delta M/M\ \gamma^2 \Delta\ t/t = 0.02$ at E = 2.1 GeV/nucleon.

4. Data Acquisition

All data from the particle telescopes, the wire chambers, and the scintillation counters are recorded on magnetic tape. A CAMAC system interfaces all data sources to a PDP-11/Disc Oriented System.

REFERENCES

1. H. H. Heckman, High Energy Heavy Ions: A New Area for Physics Research. Presented at 5th International Conference on High-Energy Physics and Nuclear Structure, Uppsala, Sweden, June 18-22, 1973.

2. P. J. Lindstrom, D. E. Greiner, H. H. Heckman, Bruce Cork, and F. S. Bieser, "Isotope Production Cross Sections from the Fragmentation of ^{16}O and ^{12}C at Relativistic Energies", LBL-3650, February 1975 (to be published).

3. D. E. Greiner, P. J. Lindstrom, H. H. Heckman, Bruce Cork, and F. S. Bieser, "Momentum Distribution of Isotopes Produced by Fragmentation of Relativistic ^{12}C and ^{16}O projectiles", Phys. Rev. Letters 35 152 (1975).

4. H. H. Heckman, D. E. Greiner, P. J. Lindstrom, and F. S. Bieser, Fragmentation of Nitrogen-14 Nuclei at 2.1 GeV per Nucleon, Science 174 1130 (1971).

5. H. H. Heckman, D. E. Greiner, P. J. Lindstrom, and F. S. Bieser, Fragmentation of ^{14}N Nuclei at 29 GeV; Inclusive isotope spectra at 0^{o}, Phys. Rev. Letters 28, 926 (1972).

6. D. E. Greiner, P. J. Lindstrom, F. S. Bieser, and H. H. Heckman, "A Facility for Calibrations and Short Experiments with Heavy Ions at the Bevatron", Nuc. Inst. and Meth., 116, 21, 1974.

7. H. H. Heckman, D. E. Greiner, R. Albert, P. J. Lindstrom, and F. S. Bieser, University of California Space Science Laboratory Report, Series 9 Issue 28, April 1968.

8. D. E. Greiner, A versatile, high-resolution particle identifier - theory, Nuclear Instruments and Methods 103, 291 (1972).

FIGURE CAPTIONS

Fig. 1 Magnetic spectrometer for the 0^{o} - fragmentation experiment. Fragments of heavy ion beam (^{16}O) produced within 12.5 mr of the beam direction are focused along guide rail according to charge and momentum.

Fig. 2 Rigidity (P/z) spectrum for the carbon isotopes produced by the fragmentation of ^{16}O nuclei at 2.1 GeV/nucleon.

Fig. 3 Plan of magnetic spectrometer beam lay-out. First focus of extracted beam is at F1. Target is placed at second focus F2. The spectrometer from F2 to F3 consists of two quadrupole doublets, Q1 and Q2 and two bending magnets, M1 and M2. A vacuum chamber is installed between M2 and F3. Detectors are at F3.

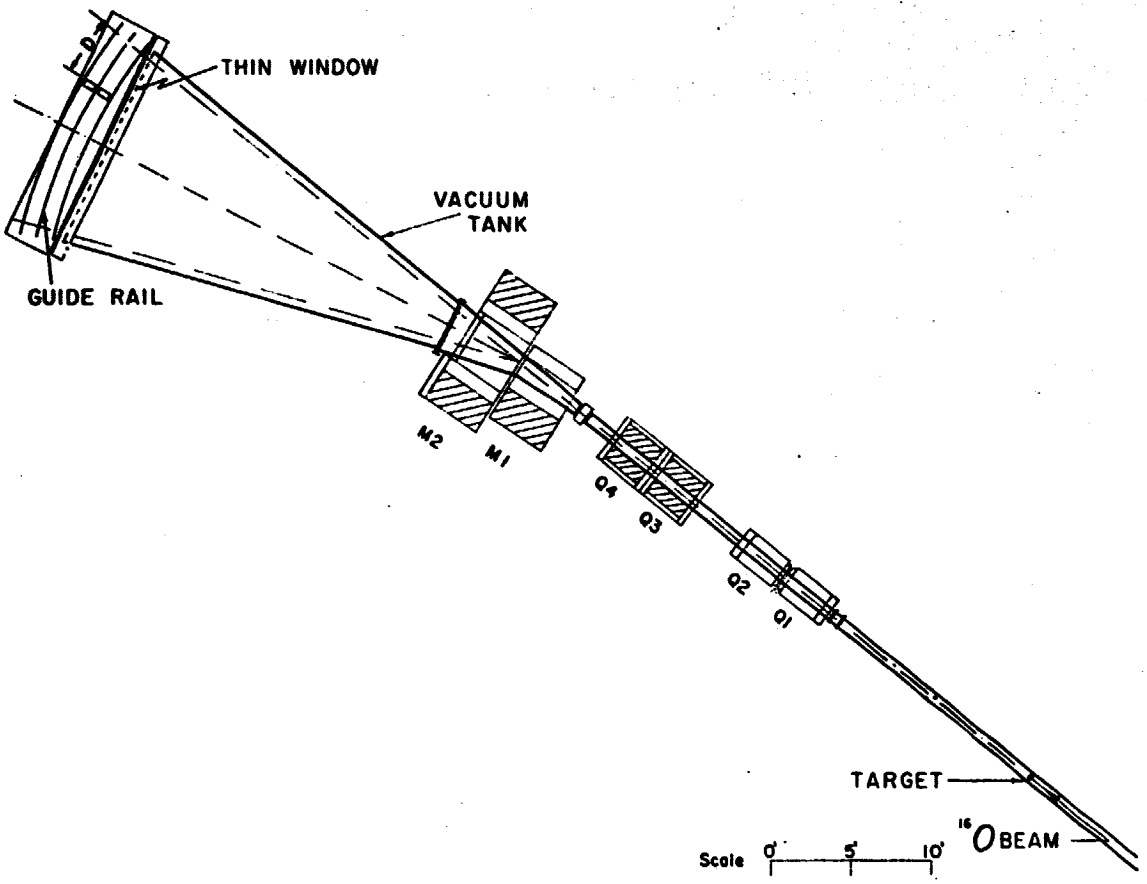
THIN WINDOW
VACUUM TANK
GUIDE RAIL
M2
M1
Q4
Q3
Q2
Q1
TARGET
16O BEAM
Scale
0'
5'
10'

Fig. 1

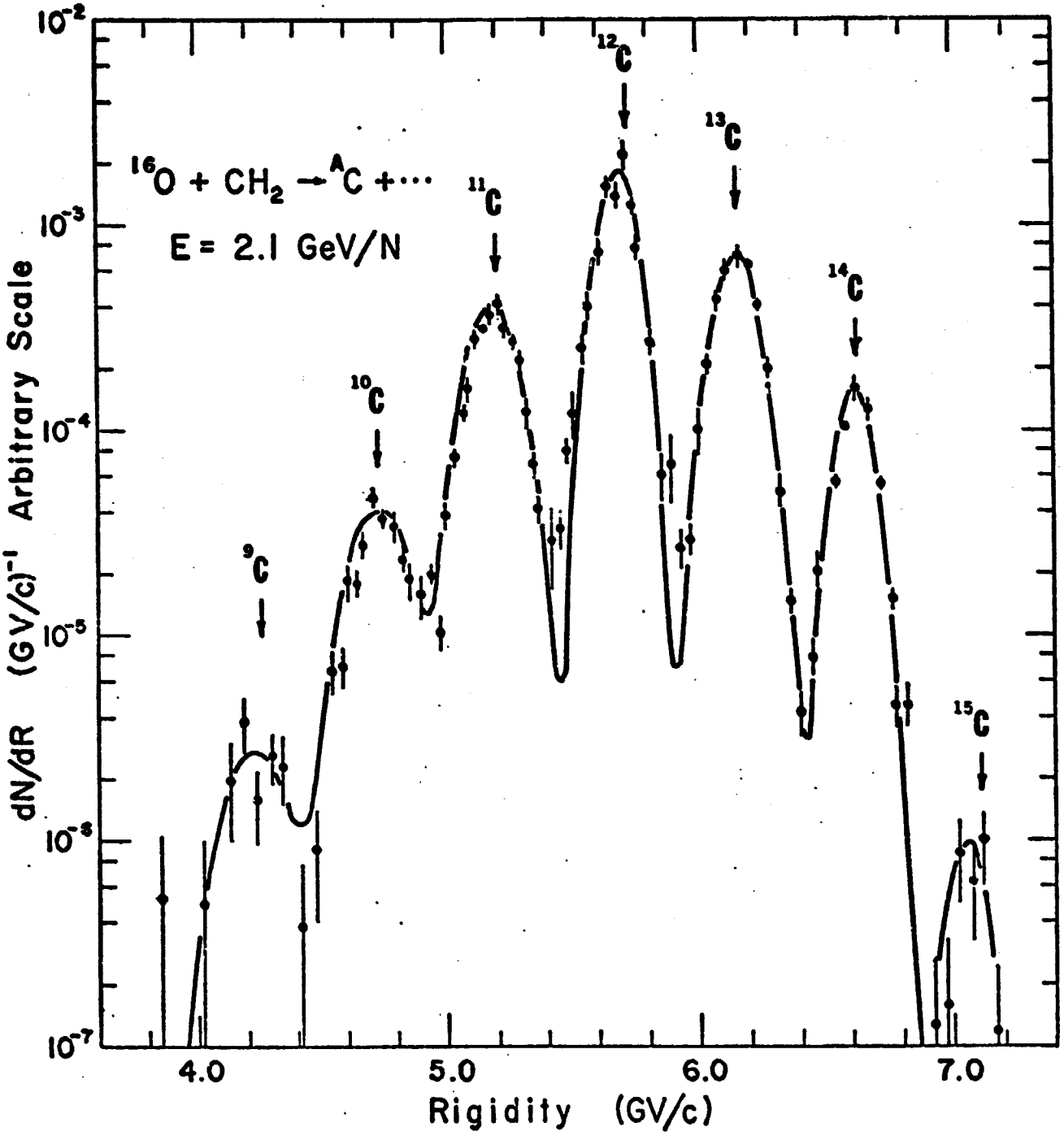
$^{16}O + CH_2 \rightarrow {}^{A}C + \cdots$
E = 2.1 GeV/N
^{9}C
^{10}C
^{11}C
^{12}C
^{13}C
^{14}C
^{15}C
dN/dR (GV/c)$^{-1}$ Arbitrary Scale
10^{-2}
10^{-3}
10^{-4}
10^{-5}
10^{-6}
10^{-7}
4.0
5.0
6.0
7.0
Rigidity (GV/c)

Fig. 2

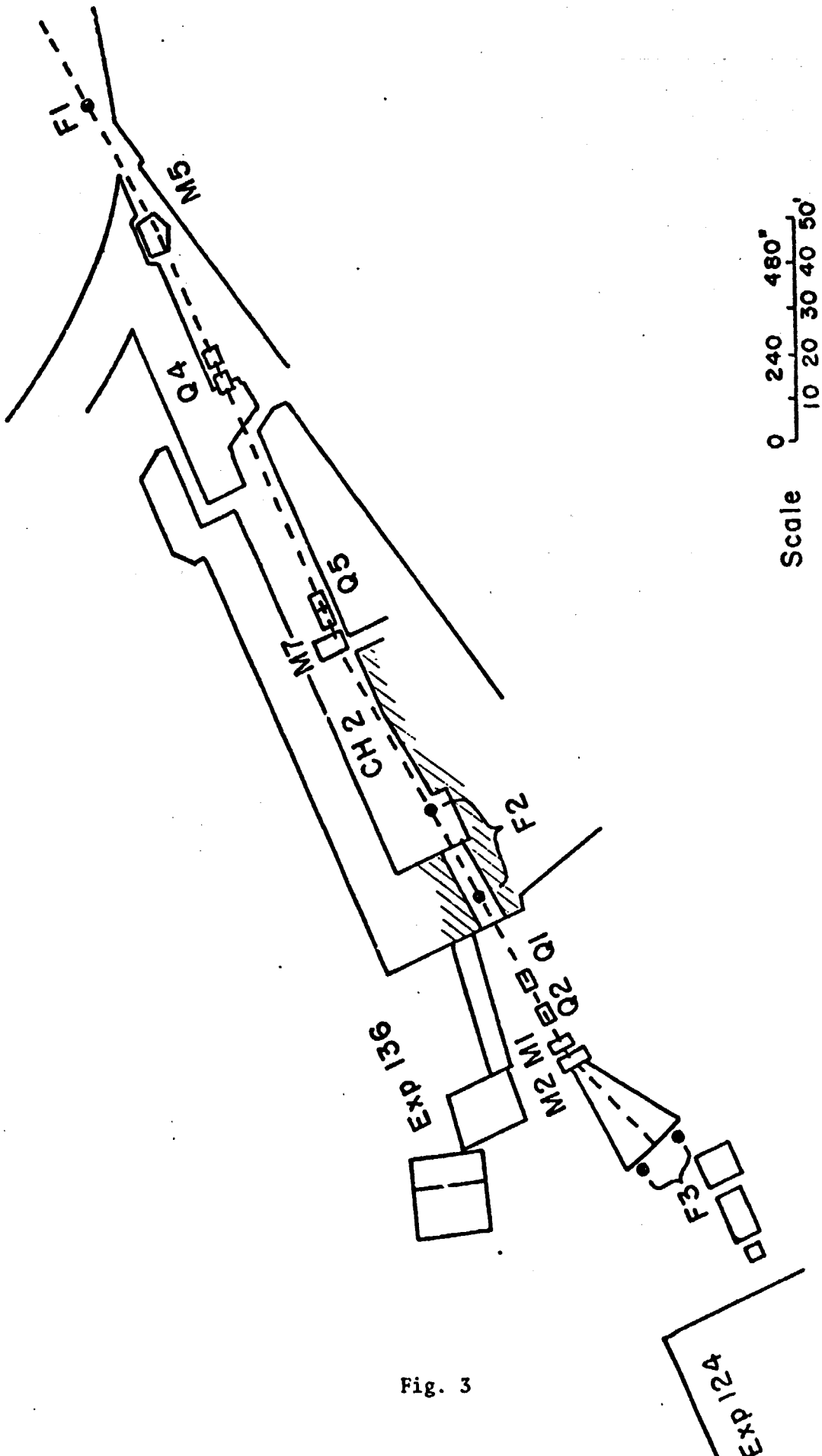
F1
M5
O4
O5
M7
CH 2
F2
M2
M1
O2
O1
Exp 136
F3
Exp 124
Scale
0 240 480'
10 20 30 40 50'

Fig. 3

APPENDIX I

Submitted to Physical Review Letters March, 1975

LBL-3651

MOMENTUM DISTRIBUTIONS OF ISOTOPES PRODUCED BY FRAGMENTATION OF RELATIVISTIC ^{12}C AND ^{16}O PROJECTILES.*

D. E. Greiner, P. J. Lindstrom, H. H. Heckman,

Bruce Cork and F. S. Bieser

Lawrence Berkeley Laboratory and Space Sciences Laboratory
University of California, Berkeley, California 94720

ABSTRACT

Presented are results on the momentum distributions for isotopes produced within 12.5 mr of the beam direction from the fragmentation of beams of ^{12}C at 1.05 and 2.1 GeV/n and ^{16}O at 2.1 GeV/n. In the projectile rest frame the momentum distributions are, typically, Gaussian shaped. For fragments $A \geq 2$, the momentum distributions are isotropic, depend on fragment and beam, and have no significant correlation with target mass or beam energy.

We present here the first comprehensive measurements of the momentum distributions for isotopes produced by the fragmentation of heavy-ion beams at the Bevatron. These results apply to the fragmentation of ^{12}C nuclei with energies 1.05 and 2.1 GeV/n, and ^{16}O at 2.1 GeV/n. The evaluation of the isotopic production cross sections given by Lindstrom et. al.[1] is based on these data.

The momentum and cross section measurements were performed using a single-focusing magnetic-spectrometer with a half-angle acceptance of 12.5 mr about zero degrees.[2] Targets were Be, CH_2, C, Al, Cu, Ag and Pb. The charge and mass of the fragments were obtained by measuring their rigidity (Pc/Ze), energy loss in solid state detectors, and time-of-flight. Particle trajectories were determined with multiple-wire proportional chambers. The longitudinal and transverse momenta, $P_{\parallel}$ and $P_{\perp}$, were obtained from the rigidity and direction of the particle at the focal plane of the spectrometer. The rigidity range was scanned in 0.1 GV steps from 0.8 to 10.2 GV for the 2.1 GeV/n ^{12}C and ^{16}O beams and 0.2 to 6.3 GV for the ^{12}C beam at 1.05 GeV/n. Because the velocities of the projectile fragments are near the beam velocity,[3] these rigidity ranges allowed us to observe all particles produced having a mass to charge ratio, A/Z, between 0.2 and 3.4.

For each isotope the longitudinal-momentum distribution, in the projectile rest frame, was fit to a Gaussian dependence on $P_{\parallel}$. The fitted variables are amplitude, central momentum, $\langle P_{\parallel} \rangle$, and standard deviation $\sigma_{P_{\parallel}}$. Fig. 1 illustrates the Gaussian

fit and the variables $\langle P_{\parallel} \rangle$ and $\sigma_{P_{\parallel}}$ for the case of ^{10}Be produced by the fragmentation of 2.1 GeV/n ^{12}C on a Be target. It is emphasized that this analysis applies to the central portion of the momentum spectrum in the projectile rest frame. The fits were restricted to the interval -400 MeV/c to +400 MeV/c which cover typically 1 to 2 decades in the magnitude of the differential cross section. The spectra of all the observed fragments exhibit properties similar to those shown in Fig. 1, namely: the momentum distributions have standard deviations of only 50-200 MeV/c, and the average momentum is slightly negative relative to the projectile.

We find that the Gaussian shape provides a good fit to the observed spectra for all isotopes regardless of beam, energy, or target except for the hydrogen isotopes. The ^{2}H and ^{3}H spectra are fit by a Gaussian curve in the region $-300 \leq P_{\parallel} \leq 400$ MeV/c, but exhibit an enhancement for $P_{\parallel} \leq -300$ MeV/c. The ^{1}H spectrum cannot be fit by a Gaussian shape in the central region $|P_{\parallel}| \leq 150$ MeV/c. In this region a fit to the ^{1}H spectrum is obtained with the exponential relation $d\sigma/dp_{\parallel} \propto \exp(-|P_{\parallel}|/65)$.

The $P_{\perp}$ distributions are based on the measurement of small angles and are less accurate than the $P_{\parallel}$ values. From measurements of the widths of the $P_{\perp}$ distribution for $A \geq 2$ fragments, we find $\sigma_{P_{\perp}} = \sigma_{P_{\parallel}}$ to an accuracy of 10% which indicates that these fragments are produced isotropically.

If these reactions are examples of limiting fragmentation, the large separation in rapidity between the target and the fragment distributions requires the shape of the momentum distributions be independent of target and beam energy.[4] For all

reactions the target and energy dependence of the variables $\langle P_{\parallel} \rangle$ and $\sigma_{P_{\parallel}}$ were examined. Within the accuracy of this experiment we conclude there is no dependence on target mass above the 5% level for $\sigma_{P_{\parallel}}$ and above the 10% level for $\langle P_{\parallel} \rangle$. Because of this observed target independence we shall refer to the target-averaged values of $\sigma_{P_{\parallel}}$ and $\langle P_{\parallel} \rangle$ in the remainder of this Letter. To determine if $\sigma_{P_{\parallel}}$ and $\langle P_{\parallel} \rangle$ are independent of energy we compare the measurements of these variables for the ^{12}C beam at 2.1 and 1.05 GeV/n. The weighted averages over all fragments of the quantities $\sigma_{P_{\parallel}}$ (2.1 GeV/n)/$\sigma_{P_{\parallel}}$ (1.05 GeV/n) and $\langle P_{\parallel} \rangle$(2.1 GeV/n)-$\langle P_{\parallel} \rangle$(1.05 GeV/n) are 1.02±0.02 and -1.0±2.0 MeV/c, respectively. This independence of beam energy and target lead to the conclusions that the ^{12}C reactions satisfy the limiting fragmentation hypothesis and the limiting energy region is reached before 1.05 GeV/n.

In the limiting energy region the fragment distributions depend on the identity of the projectile and fragment.[4] We begin discussion of this dependence by presenting in Table I the measured values of $\sigma_{P_{\parallel}}$ and $\langle P_{\parallel} \rangle$ for all fragments produced with sufficient signal. In Fig. 2 we have plotted the values of $\sigma_{P_{\parallel}}$ for ^{16}O at 2.1 GeV/n versus the fragment mass in amu. The charge of each fragment is used as the plotting symbol. In an attempt to parameterize the mass dependence we have fit the data to the function $\sigma^2_{P_{\parallel}}(B,F) = 4\,\sigma_o^2 F(B-F)/B^2$ where B and F are the mass numbers of the beam and fragment nuclei respectively, and σ_o is the fitted variable. The best-fit curve for ^{16}O is shown in Fig. 2. The fitted values of σ_o for all beams are listed in

Table II. Although the parabola shape displays the general trend of the data, in no case does it provide a good fit to the observed values of $\sigma_{P_\parallel}$.[5] The poor fit is demonstrated by the fact that 50% of the data points are over two standard deviations from the curve. Particularly striking is the observation that the same complex variation of $\sigma_{P_\parallel}$ with fragment mass is exhibited by both the ^{12}C and ^{16}O fragments, indicating nuclear structure effects are important variables determining the $\sigma_{P_\parallel}$ values.

The values of $<P_\parallel>$ have an approximately linear relationship on $\sigma_{P_\parallel}$. In Fig. 3 we show the data representing all fragments from ^{12}C and ^{16}O projectiles at 2.1 GeV/n to exhibit this linear dependence. The general shifts in the momentum distributions toward velocities less than the beam correspond to small energy transfers to the fragment, typically < 130 KeV in the projectile frame. The obvious exceptions are reactions involving charge exchange, such as $^{12}C \rightarrow {}^{12}N$, and charge exchange plus loss of a nucleon, e.g., $^{16}O \rightarrow {}^{15}C$. The reactions involving charge exchange generally have larger negative values of $<P_\parallel> \simeq -100$ MeV/c. Calculation of the missing mass in these reactions gives values approximately 200 MeV/c^2 after subtraction of the target mass. Thus the data are consistent with the assumption that the charge exchange reactions proceed via pion production, for example $^{12}C \rightarrow {}^{12}N + \pi^-$.

The fragmentation of heavy ions at relativistic energies is a relatively new field of research. There is, therefore, no well developed theory to compare with experimental results. Preliminary attempts, however, have been made to understand the momentum dis-

tribution widths. Several authors have derived a dependence of $\sigma_{P_\parallel}$ on fragment mass of the form $\sigma^2_{P_\parallel} \propto F(B-F)$. The validity and implications of these theories can be determined by comparison with the values of σ_o measured by this experiment. A parabolic dependence of $\sigma^2_{P_\parallel}$ on fragment mass was first predicted by Wenzel,[6] later by Lepore and Riddell,[7] and indirectly by Feshbach and Huang[8] as extended by Goldhaber.[9] In general the parabolic shape arises when one assumes: i) the fragment momentum distributions are essentially those in the projectile nucleus, ii) that there are no correlations between the momenta of different nucleons, and iii) momentum is conserved. The work of Lepore and Riddell[7] is a quantum mechanical calculation that employs the sudden approximation with shell-model wave functions to predict $\sigma_o^2 = \frac{1}{8} m_p B^{1/3} \left[45B^{1/3} - 25\right]$. This expression, where m_p is the proton mass, gives qualitative agreement with the measured values as shown in Table II. Feshbach and Haung[8] assume sudden emission of virtual clusters and relate σ_o to the Fermi momentum of the projectile, P_f. Using the formulation due to Goldhaber,[9] the relation between P_f and σ_o is $\sigma_o^2 = \frac{1}{20} P_f^2 B^2/(B-1)$. The values of P_F determined by quasielastic electron scattering[10] give predicted values of σ_o that are generally 25% higher than the measured values as shown in Table II. An interesting point to note here is that through the predicted relationship between σ_o and P_f, this experiment measures the projectile Fermi momentum via nuclear fragmentation (see Table II). By assuming the projectile has come to thermal equilibrium at an excitation temperature T, Goldhaber[9] has shown that the parabolic shape is again predicted and relates

σ_o to the excitation energy per nucleon by the equation $kT=4\sigma_o^2/m_nB$, where k is Boltzmann's constant and m_n is the nucleon mass. The measured values of σ_o then reflect excitation energies which we have listed in Table II along with the average binding energies per nucleon as determined by the projectile masses.[11,12] Because our measured excitation energies are essentially the binding energy per nucleon of the projectiles, we again conclude that the fragmentation process which results in bound fragments involves very little energy transfer between the target and fragment.

Based on our initial fragmentation studies the following picture emerges: when heavy ions at high velocity interact with matter, a fraction of the reactions emit fragments having essentially the same velocity as the original ion. The probability for this occurrence depends on the target nucleus, ranging from 90% for ^1H to 30% for Pb.[1] Interactions of this type account for the total fragmentation cross sections for fragments $A\geq 2$. In these reactions the $(A\geq 2)$ fragments are emitted isotropically with Gaussian momentum distributions in the projectile frame. These distributions are independent of target mass and projectile energy, which are basic requirements of the limiting fragmentation hypothesis. Energy transfers to the fragment are small; in fact, the observed excitation energies are remarkably close to the binding energy of the projectile. Finally there is strong and recurring evidence in our data of effects attributable to nuclear structure in both the fragment-momentum distributions and the fragmentation cross sections.

We thank the Bevatron operations staff, under H. A. Grunder and R. J. Force, for their support and effort during this experiment. We commend E. E. Beleal, D. M. Jones, and C. P. McParland for their computer programming efforts and data handling, and R. C. Zink for electronic component construction.

FOOTNOTES REFERENCES

* Work performed under auspices of the U. S. Atomic Energy Commission and the National Aeronautics and Space Administration, Grant NGR 05-003-513.

1. P. J. Lindstrom, D. E. Greiner, H. H. Heckman, Bruce Cork and F. S. Bieser, UCRL 3650 (submitted to Phys. Rev. Lett.)

2. D. E. Greiner, P. J. Lindstrom, F. S. Bieser and H. H. Heckman, Nucl. Inst. and Meth. 116, 21 (1974).

3. H. H. Heckman, D. E. Greiner, P. J. Lindstrom and F. S. Bieser, Phys. Rev. Lett. 28, 926 (1972).

4. W. R. Frazer, et. al., Rev. Mod. Phys. 44, 284 (1972).

5. Preliminary results based on eight isotopes not including ^{1}H indicated $\sigma_{P_{\|}} \approx 140$ MeV/c, independent of mass (H. H. Heckman, 5th, Intl. Conf. High-Energy Phys. Nucl. Struct., Uppsala, June 1973.) Based on all the data presented here, a constant value of $\sigma_{P_{\|}}=137$ MeV/c gives a goodness-of-fit comparable to that obtained with a parabolic dependence, $\chi^2=1370$ if $\sigma_{P_{\|}}=137$ MeV/c versus $\chi^2=600$ for the parabola with 32 degrees of freedom.

6. W. A. Wenzel, LBL Heavy Ion Seminar, 1973 (unpublished).

7. J. V. Lepore and R. J. Riddell, Jr., LBL 3086, 1974 (unpublished).

8. H. Feshbach and K. Huang, Phys. Lett. 47B, 300 (1973).

9. Alfred S. Goldhaber, Phys. Lett. 53B, 306 (1974). The fragmentation problem has also been studied by Fumiyo Uchiyama, LBL 3318, 1974 (unpublished).

10. E. J. Moniz, I. Sick, R. R. Whitney, J. R. Ficenec, R. D. Kephart and W. P. Trower, Phys. Rev. Lett. 26, 445 (1971).

11. Particle Data Group, Phys. Lett. 50B (1974).

12. C. M. Lederer, J. M. Hollander, and I. Perlman, Table of Isotopes, John Wiley & Sons Inc., New York, N. Y. (1967).

Table I. MOMENTUM DISTRIBUTION WIDTHS AND CENTERS (MeV/c)[a]

BEAM	ENERGY	SECONDARY Z_F	SECONDARY A_F	$\sigma_{P_\parallel}$	$\langle P_\parallel \rangle$
^{16}O	2.10 GeV/n	1	1[b]	71± 6	-1± 5
		1	2	134± 3	-23± 2
		1	3	150± 3	-41± 5
		2	3	156± 2	-38± 3
		2	4	131± 1	-27± 3
		2	6	167±20	-40±10
		3	6	141± 7	-33± 7
		3	7	163± 4	-46± 6
		3	8	170±13	-24±12
		3	9	188±15	-63±31
		4	7	166± 2	-45± 9
		4	9	166± 7	-47± 7
		4	10	159± 6	-65± 6
		4	11	197±20	-73±27
		5	8	175±22	-57±11
		5	10	175± 7	-40± 7
		5	11	160± 2	-53± 3
		5	12	163± 8	-59±10
		5	13	166±10	-67±23
		6	10	190± 9	-32±15
		6	11	162± 5	-45±13
		6	12	120± 4	-25± 6
		6	13	130± 3	-33± 7
		6	14	125± 3	-38± 7
		6	15	125±19	-132±25
		7	12	153±11	-49±28
		7	13	134± 2	-35± 4
		7	14	112± 3	-27± 3
		7	15	95± 3	-21± 6
		7	16	59±11	-110±15
		8	13	143±19	-57±26
		8	14	99± 6	-31± 7
		8	15	99± 3	-23± 3
^{12}C	2.10 GeV/n	1	1[b]	67± 5	0± 3
		1	2	134± 4	-27± 3
		1	3	138± 5	-48± 4
		2	3	145± 8	-31± 4
		2	4	129± 1	-25± 4
		2	6	136± 7	-29±15
		3	6	127± 7	-33±10
		3	7	144± 2	-40± 7
		3	8	159± 7	-43±12
		3	9	161± 9	-35±17
		4	7	145± 2	-49± 6
		4	9	133± 3	-38± 9
		4	10	129± 4	-30± 8
		4	11	155±40	-102±82
		5	8	151±16	-39±12
		5	10	134± 3	-35± 7
		5	11	106± 4	-23± 9
		5	12	63± 9	-96±14
		6	9	147±21	-43±30
		6	10	121± 6	-42±11
		6	11	103± 4	-40± 9
		7	12	56±14	-100±11
^{12}C	1.05 GeV/n	1	1[b]	63± 4	13± 4
		1	2	113±11	-13±12
		1	3	162±19	-25±13
		2	3	132±19	-32± 2
		2	4	125± 3	-27± 2
		2	6	142±20	-32±14
		3	6	122±10	-28± 7
		3	7	142± 7	-44± 4
		3	8	160±26	-35±14
		3	9	139±19	-43±20
		4	7	140± 6	-33± 5
		4	9	131± 9	-35± 5
		4	10	125±11	-37± 5
		4	11	103±37	-104±43
		5	8	139±12	-61±20
		5	10	135± 9	-35± 8
		5	11	102±11	-30± 4
		5	12	88±17	-112±31
		6	9	147±20	-28±17
		6	10	126± 8	-46± 5
		6	11	105±10	-43± 4
		7	12	93±19	-55±19

[a] PROJECTILE FRAME PARALLEL MOMENTUM AVERAGED OVER ALL TARGETS (ERRORS INCLUDE SYSTEMATIC AND STATISTICAL CONTRIBUTIONS)
[b] NON-GAUSSIAN DISTRIBUTION

Table II. Comparison with theory and experiment of parameters related to a $\sigma_{P_\parallel}$ mass dependence of the form $\sigma_{P_\parallel}^2 = 4\sigma_o^2 F(B-F)/B^2$. Derived quantities are Fermi momentum $P_f = 20\sigma_o^2(B-1)/B^2$ and average excitation energy $kT = 4\sigma_o^2/m_n 3$.

		Projectile		
Parameter	Origin	^{16}O 2.1 GeV/n	^{12}C 2.1 GeV/n	^{12}C 1.05 GeV/n
σ_o(MeV/c)	this expt.	171±3	147±4	141±5
"	sudden approximation[7]	162	145	145
"	virtual clusters[8]	212	179	179
P_f(MeV/c)	this expt.	185±3	182±5	174±6
"	electron scattering[10]	230	221	221
kT(MeV/n)	this expt.	7.8±0.3	7.7±0.4	7.1±0.5
average binding energy (MeV/c)	mass measurements[11,12]	8.0	7.7	7.7

Figure Captions

1. The projectile-frame parallel-momentum distribution for ^{10}Be fragments from ^{12}C at 2.1 GeV/n on a Be target. The mean momentum $\langle P_{\parallel} \rangle = -30$ MeV/c and standard deviation $\sigma_{P_{\parallel}} = 129$ MeV/c are indicated. The curve shown is the best fit to a Gaussian momentum distribution.

2. Plotted are the target-averaged widths $\sigma_{P_{\parallel}}$ of the projectile-frame parallel-momentum distributions, in MeV/c, versus fragment mass in amu. The plotted symbol indicates the charge of the fragment. These data represent fragments of ^{16}O at 2.1 GeV/n. The asterisk denotes that the ^{1}H is a non-Gaussian momentum distribution and we have used the central region of this distribution to evaluate $\sigma_{P_{\parallel}}$. The parabola represents the best fit to the data.

3. Dependence of $\langle P_{\parallel} \rangle$ on $\sigma_{P_{\parallel}}$ for all fragments observed from ^{12}C and ^{16}O beams. The average linear relationship is $\langle P_{\parallel} \rangle = -0.5\ \sigma_{P_{\parallel}} + 30$. The divergent points with $\langle P_{\parallel} \rangle \simeq \pm 100$ MeV/c are reactions involving charge exchange.

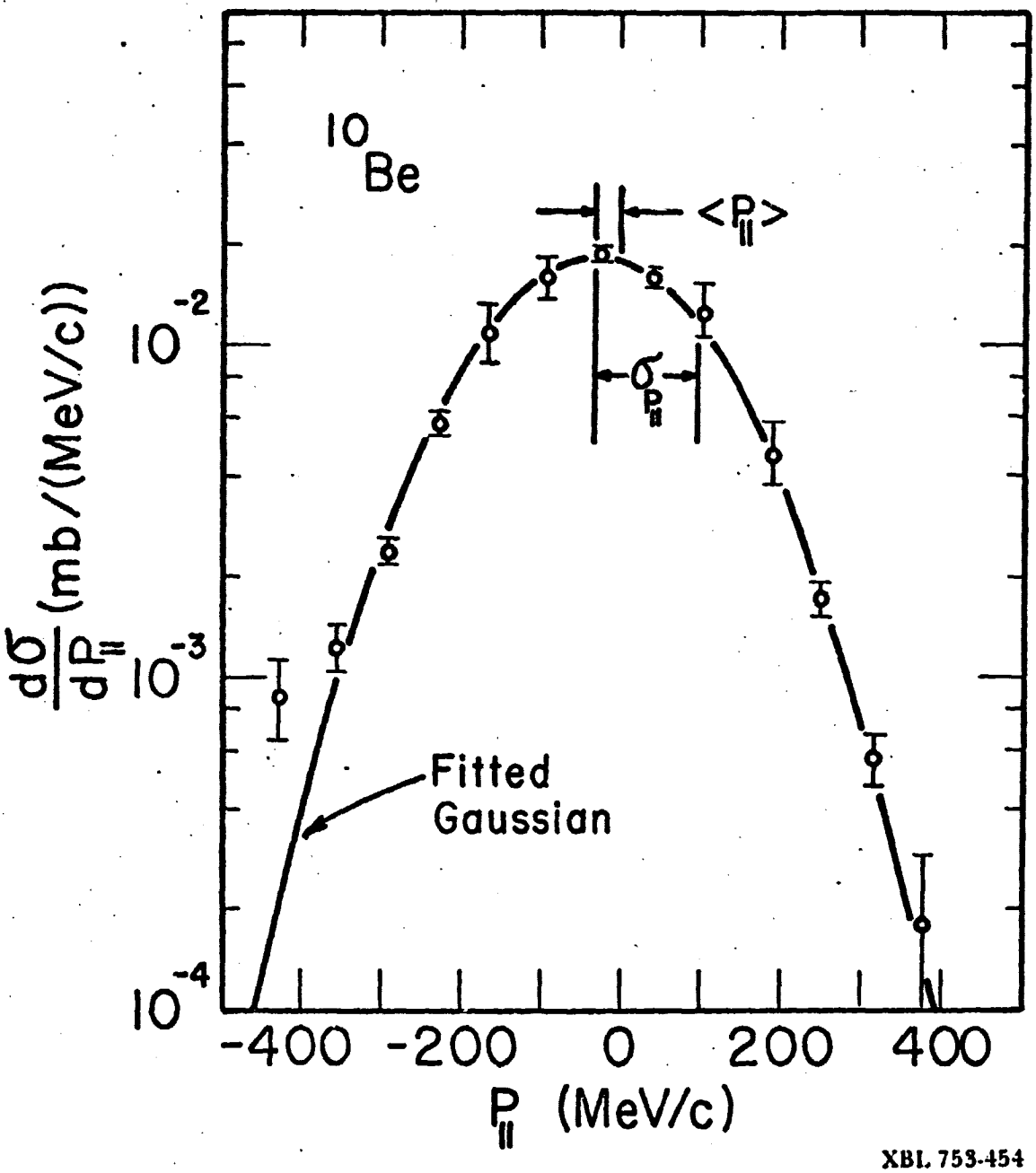
10 Be
<P∥>
σ P∥
Fitted Gaussian
dσ/dP∥ (mb/(MeV/c))
10^-2
10^-3
10^-4
-400
-200
0
200
400
P∥ (MeV/c)
XBL 753-454

Fig. 1

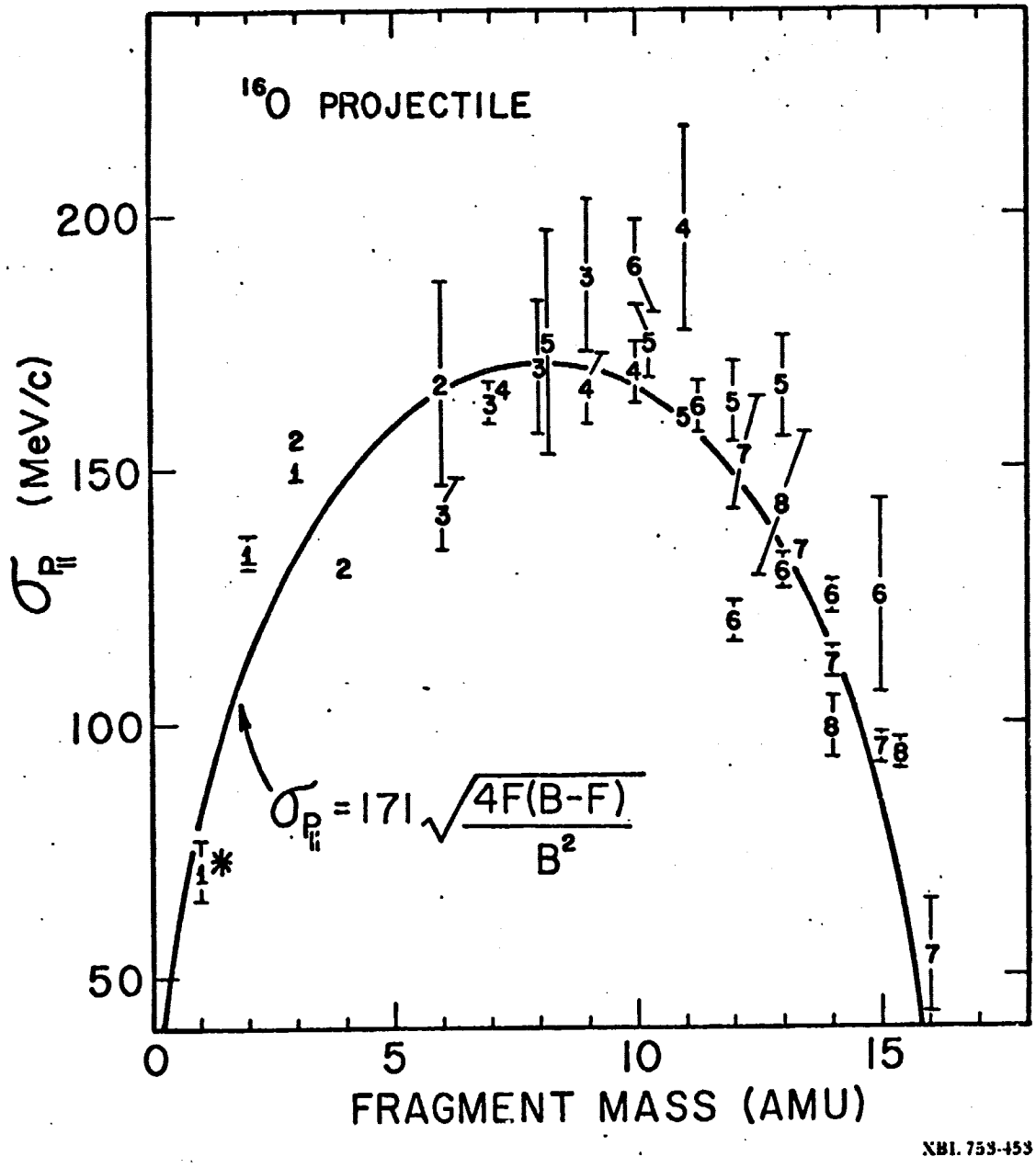
^{16}O PROJECTILE
200
150
100
50
$\sigma_{P_{\parallel}}$ (MeV/c)
$\sigma_{P_{\parallel}} = 171\sqrt{\frac{4F(B-F)}{B^2}}$
0
5
10
15
FRAGMENT MASS (AMU)
XBL 753-453

Fig. 2

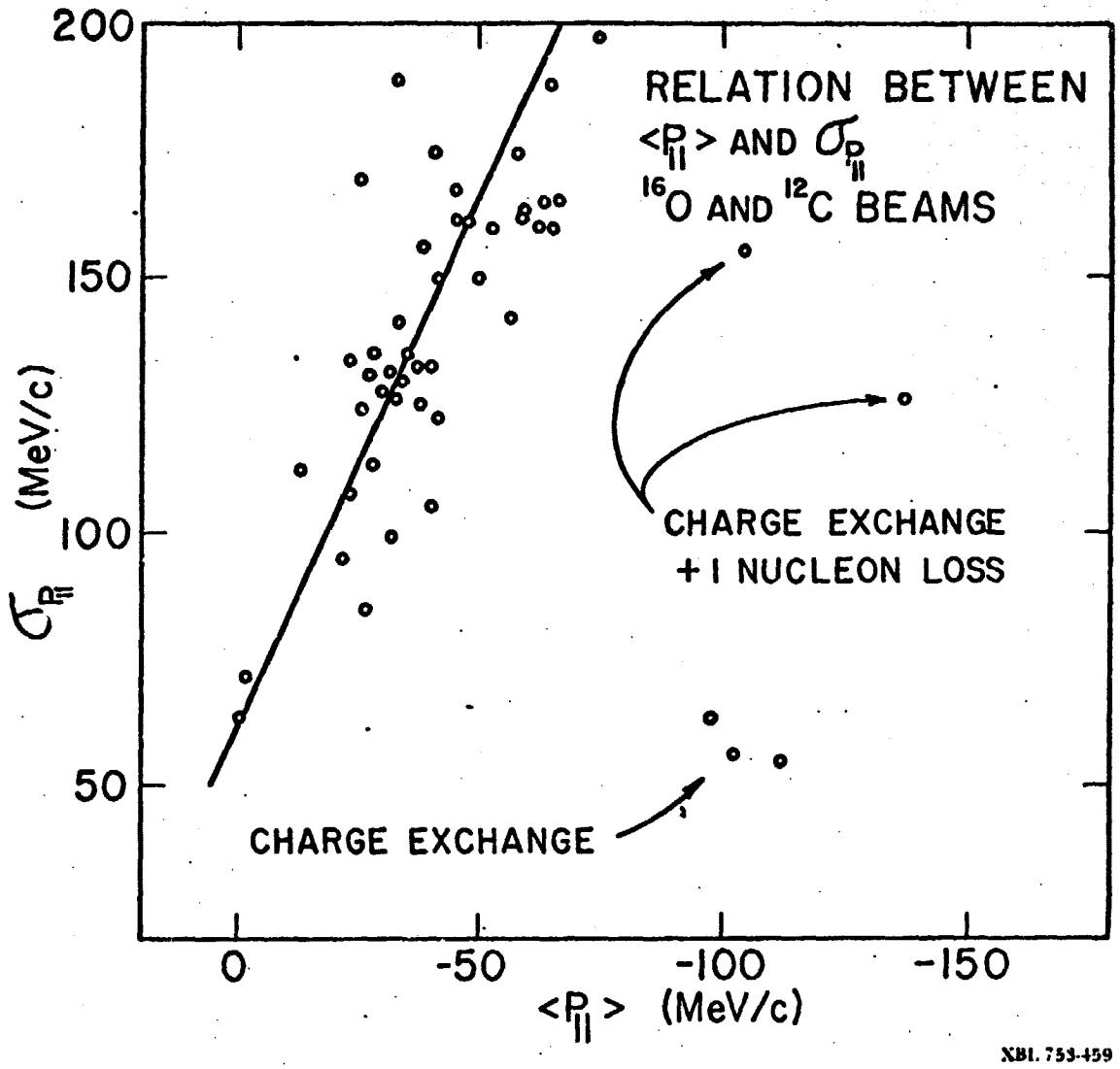
RELATION BETWEEN
<P|| > AND σP||
16O AND 12C BEAMS
CHARGE EXCHANGE
+1 NUCLEON LOSS
CHARGE EXCHANGE
200
150
100
50
0
-50
-100
-150
σP|| (MeV/c)
<P|| > (MeV/c)
XBL 753-459

Fig. 3

APPENDIX II

ISOTOPE PRODUCTION CROSS SECTIONS FROM THE FRAGMENTATION OF ^{16}O and ^{12}C AT RELATIVISTIC ENERGIES.*

P. J. Lindstrom, D. E. Greiner, H. H. Heckman

Bruce Cork and F. S. Bieser

Lawrence Berkeley Laboratory and Space Sciences Laboratory

University of California, Berkeley, California 94720

ABSTRACT

The 0-degree fragmentation products of ^{16}O and ^{12}C at 2.1 GeV/n and ^{12}C at 1.05 GeV/n have been measured for targets ranging from H to Pb. We present a total of 464 partial-production cross sections for 35 isotopes. The cross sections are energy independent and can be factored into beam-fragment and target terms. The target factor, $\gamma_T \sim A_T^{\frac{1}{4}}$, and other evidence, imply the isotopes are produced in peripheral interactions.

Submitted to Physical Review Letters February, 1975

We have measured at the Bevatron the single-particle inclusive spectra of all isotope fragments of ^{16}O and ^{12}C at 2.10 GeV/n and of ^{12}C at 1.05 GeV/n. The targets were Be, CH_2, C, Al, Cu, Ag, and Pb. The hydrogen target data were obtained by CH_2-C subtraction. The measurements were limited to secondaries produced within a ±12.5 mr cone about 0-deg from the direction of the primary beam. Secondary momenta were limited to rigidities (pc/Ze) less than 9 GV. All secondaries with lifetimes greater than 10^{-8} seconds and production cross sections greater than 10μb were observed. The spectrometer system[1,2] resolved charge, mass, and momentum for all secondaries at any given spectrometer rigidity setting.

The observed longitudinal and transverse momentum spectra of the isotope fragments, when transformed to the projectile rest frame, have Gaussian distributions centered near 0-MeV/c, with standard deviations (S.D) ∿60-200 MeV/c. The cross sections presented in Table I were obtained by integrating these momentum distributions. Since the observed fragments were confined to a 12.5 mr cone, it was necessary to extrapolate the transverse momentum distributions to obtain total partial cross sections. Except for the $Z \leqslant 2$ fragments, the 12.5 mr region accounted for 70%-100% of the total cross sections. Both observed momentum systematics[2] and measured angular distributions in nuclear emulsion[3] give confidence in this extrapolation for $A \geqslant 2$ secondaries. The proton momentum distribution is non-Gaussian and no attempt was made to extrapolate this distribution to estimate total production cross sections. The cross sections are corrected for beam and secondary fragmentation in the targets, vacuum windows, and scintillators, as well as for interactions in the Si(Li) detectors. Corrections are made for focus, geometry, misalignment, and multiple

secondaries with the same rigidity. Focus, solid angle, and target-loss errors give a base 4-8% systematic error which is included in Table I [4] errors. The momentum distributions show the cross sections σ_{BT}^{F}, where beam B interacts with target T to produce fragment F, are measurements of fragments of the projectile, and not fragments of the target. No fragments were observed with velocities much less than beam velocity. No nucleon-pickup isotopes were observed. Between 30% (Pb target) and 90% (H target) of all beam charge is accounted for in Table I σ_{BT}^{F}. The missing charge is principally in large momentum transfer protons.

The σ_{BT}^{F}, for a hydrogen target, can be compared with cross sections of proton-nucleus interactions at high energies. At proton energies $\geq$ 600 MeV, 42 measured cross sections for 15 different secondaries have been compiled.[5,6] Comparing Table I data with the proton measurements, 24 are within 1 S.D., 9 are within 1-2 S.D., 7 are 2-3 S.D., and 2 are 3-4 S.D. The two cross section measurements 3-4 S.D. from our data are $p + {}^{16}O \rightarrow {}^{10}C + ---$ at $T_p = 1$ GeV and $p + {}^{16}O \rightarrow {}^{10}Be + ---$ at 600 MeV. Comparison of our results can also be made with the semi-empirical model by Silberberg and Tsao[8], which is based on the proton-nucleus data set mentioned above. We find the experimental values σ_{BT}^{F} above 1 mb listed in Table I are greater than those given by the Silberberg and Tsao model by an average of 22%, with a S.D. of 37%.

Target factorization is expected both from high energy phenomenology[9] and from an impulse approximation model of nuclear fragmentation.[10] We observe that the cross sections can be factored, $\sigma_{BT}^{F} = \gamma_{B}^{F} \gamma_{T}$, where γ_{B}^{F} depends on the projectile and fragment and γ_{T} is the target factor (Fig. 1). This result confirms, and significantly extends, the first experiments on the fragmentation of relativistic nuclei.[11] The exceptions to strict factorization are: 1) γ_{T}

for a hydrogen target has a weak dependence on the mass of fragment A_F, i.e., $\gamma_T(H) = 0.66 + 0.028\ A_F$; and 2) γ_T for single-nucleon stripping is enchanced for heavy targets. The cross sections for single-nucleon loss on the heavier targets include a component for Coulomb dissociation, via the giant dipole resonance, in the target's virtual photon field. The Coulomb dissociation part of the cross sections can be computed[12] and subtracted from the measured σ_{BT}^F. The resultant cross sections are consistent with the target factors given in Table I. The target factors fit the data with a confidence level of 0.[illegible] and can be approximately fitted by the expression $\gamma_T = A_T^{\frac{1}{3}}$ or $\gamma_T = (A_F^{1/3} + A_T^{1/3} - 1.6)$. Both formulations for γ_T indicate the cross sections we observe are produced by peripheral interactions with the target. Neither formulation for γ_T explains the observed structure, however, particularly the result $\gamma_T(Be) > \gamma_T(C)$.

Although $A_T^{\frac{1}{3}}$ generally fits the observed data to within 10%, the confidence level for this hypothesis is less than 10^{-9}. An accurate fit to the target factor is obtained by the expression $\gamma_T = kt^n (r_T+b)$ where r_T is the measured half-density electric-charge radius and t is the measured charge skin thickness of the target.[13] The three fitted variables are: the exponent n = 0.5, b=3.0 fm, and normalizing constant k=0.26. This formula reproduces the structure in the mean target factor to an accuracy better than 2% and with a confidence level of 0.9, a great improvement over the $A^{\frac{1}{3}}$ hypothesis. Since σ_{BT}^F factors and the momenta distributions are target independent,[2] the partial differential cross sections factor -- a result expected by limiting fragmentation models. Whether γ_T contains beam-dependent terms, e.g., the sum of the radii of the beam and target nuclei, as suggested above, cannot be determined with the present data.

The energy dependence of isotope production can be examined by 1) comparing σ^F_{BT}, Table I, for the two ^{12}C-beam energies, and 2) comparing σ^F_{BT} with values from Ref. 5 & 6, measured at different energies. The carbon data for all fragments are energy independent between 1.05 and 2.10 GeV/n with a confidence level of 0.8. The error-weighted mean ratio $\sigma^F_{BT}(2.10)/\sigma^F_{BT}(1.05) = 1.01 \pm 0.01$. We have already mentioned comparison of σ^F_{BT}, for both ^{12}C and ^{16}O projectiles with previously measured target data and the agreement was generally good for energies 600 MeV/n and above. Energy independence of σ^F_{BT}, above some energy threshold, is another result expected from high energy phenomenology. A comparison of σ^F_{BT} for the same fragments and targets but different beams, ^{16}O and ^{12}C, shows, in general, a weak beam dependence in the production cross sections of all fragments in common, as long as a charge-exchange reaction is not necessary. The ratio $\sigma^F_{BT}(^{16}O)/\sigma^F_{BT}(^{12}C)$=0.4-1.35, even though the individual cross sections vary over three orders of magnitude. It is noteworthy that more than 40% of the ratios are in the interval 1.0 ± 0.15.

Production cross sections for mirror nuclei should give insight into the mechanisms which produce the observed final state. A simple evaporation model would preferentially evaporate neutrons resulting in $\sigma_N/\sigma_P \leq 1$, where σ_N/σ_P is the ratio of the production cross sections for mirror fragments, neutron rich to proton rich, of the same beam and target. Likewise, if a neutron skin extends beyond the proton surface, a stripping process would also result in $\sigma_N/\sigma_P \leq 1$. We observe that, to the contrary, $1.0 < \sigma_N/\sigma_P < 4.1$, with most values of the ratio being in the interval 1.1 to 1.7. That $\sigma_N/\sigma_P > 1$ is indicative of the effects of the binding energy of the final state fragment. For example, inspection of the mass excess vs σ^F_{BT} for isobars shows the fragment with the lower mass excess has

the higher production cross section. This dominance of final state structure in σ_{BT}^{F} complicates the choice of any simple mechanism describing the interaction process.

The patterns observed in σ_{BT}^{F} and in the momentum distributions[2] indicate simplicity in the peripheral fragmentation process. Target factorization, energy independence, and small transverse momenta are observed features of σ_{BT}^{F} and directly relate to limiting fragmentation models. The $A_T^{\frac{1}{4}}$ behavior of the target factor and the inclusion of a charge skin-thickness term in the best fit for γ_T, along with small parallel momenta widths in the beam rest frame, imply the observed fragments are the result of peripheral interactions. Neutron rich enchancement of mirror-isotope cross sections, correlations in fragment binding energies, and a surprising degree of beam independence in σ_{BT}^{F} indicate a dominance of fragment nuclear structure in the production amplitudes.

We thank the Bevatron operations staff, under H. A. Grunder and R. J. Force, for their support and effort during this experiment. We commend E. E. Beleal, D. M. Jones and C. P. McParland for their computer programming efforts and data handling, and R. C. Zink for electronic component construction.

REFERENCES

*Work performed under auspices of the U. S. Atomic Energy Commission and the National Aeronautics and Space Administration Grant NGR 05-003-513.

1. For spectrometer characteristics see D. E. Greiner, P. J. Lindstrom, F. S. Bieser, and H. H. Heckman, Nucl. Inst. and Methods, 116, 21 (1974).
2. D. E. Greiner, P. J. Lindstrom, H. H. Heckman, B. Cork, and F. S. Bieser, (submitted to Phys. Rev. Letters). LBL Report No. 3651, 1975.
3. H. H. Heckman, D. E. Greiner, P. J. Lindstrom, Hla Shwe, LBL Report No. 3656, 1975 (to be published).
4. The cross sections in Table I are available on computer cards.
5. R. Silberberg and C. H. Tsao, NRL Report No. 7593 (1973).
6. F. Yiou, G. Raisbeck, C. Perron, and P. Fontes, Conference papers, 13th International Cosmic Ray Conference, Denver, Colorado, 17-30 August 1973, Vol. I, Paper No. 251.
7. G. Raisbeck and F. Yiou, Conference papers, 13th International Cosmic Ray Conference, Denver, Colorado, 17-30 August 1973, Vol. I, Paper No. 253.
8. R. Silberberg and C. H. Tsao, Ap. J. Suppl, No. 220(I), 25, 315 (1973).
9. For a General review, see W. R. Frazer et. al., Rev. Mod. Phys. 44, 284 (1972).
10. J. V. Lepore and R. J. Riddell Jr., LBL 3086, 1974 (unpublished).
11. H. H. Heckman, D. E. Greiner, P. J. Lindstrom, and F. S. Bieser, Phys. Rev. Letters 28, 926 (1972).
12. X. Artru and G. B. Yodh, Phys. Lett. 40B, 43 (1972), (Also, report in preparation by P. L., H. H.).
13. R. Hofstadter and H. R. Collard, Nuclear radii determined by electron scattering, p. 21, Landolt-Bornstein, New series, I/2 Springer Verlag (1967).

Table I. PRODUCTION CROSS SECTIONS AND ERRORS (mb).

BEAM	ENERGY	SECONDARY Z_y	SECONDARY A_y	SECONDARY Y_0^y	N	TARGET Be	TARGET C	TARGET Al	TARGET Cu	TARGET Ag	TARGET Pb
^{16}O	2.10 GeV/n	1	1 [b]	30 ?± 3.1	37 2± 6 0		96.9± 6 2				
		1	2	222 ± 11.	152 ± 23	417 ± 37.	406 ± 34		682 ± 73.	752 ± 97	946 ±154
		1	3	78 3± 5 2	54 9±10 ?		151 ± 11.				
		2	3	72 0± 3.4	50 2± 5.7	152 ± 9.	136.± 8.				
		2	4	257 ± 13.	221 ± 20	501 ± 46	474 ± 42		748 ± 80	829 ± 98	882 ±104
		2	6	1.02± .10	728± 204		2 00± 21				
		3	6	17.5± .9	13 2± 2 4	33 0± 2 7	30 9± 2 9		61 2± 7 4	69 4± 8 5	84 0±13 4
		3	7	13.9± .7	11 1± 1 3	27 0± 1 3	26 3± 1 3	34 0± 1 8	38 7± 2 9	39 0± 3 4	39 7± 4 3
		3	8	1 23± .06	731± 149		2 58± .10		3 63± .47		
		3	9	.281± 033	341± 070		586± 067				
		4	7	11 4± .6	10 1± 1 2	22 0± 1 1	22 3± 1 1		32 0± 2 9	36 4± 3 2	43 3± 6 4
		4	8	4.68± 23	4 17± 55	9 79± 58	9 86± 51	11 2± 7	12 3± 1 1	13 8± 1 6	16 3± 2 1
		4	10	2 01± .10	2 05± 31	3 92± 27	3 90± 30		4 51± 06	5 65± 77	6 80±1 14
		4	11	.099± 014	.082± 031		.199± 033		304± 127		
		4	12	.022± 008	.045±.020		.033± 016				
		5	8	.707± 039	.580± 083	1 93± 12	1 30± 13		1 36± 30		
		5	10	10.1± .5	8.04±1 44	19 1± 1.5	20 3± 1 6		35 2± 5 5	26 6± 6 3	35 2±11 3
		5	11	13.6± .7	15 ±2 1 5	27 9± 1 4	25 9± 1 3	31 0± 1 6	35 8± 2 9	43 8± 3 4	52 8± 5 8
		5	12	1.33± .07	1 05± .17	2 79± .19	2 44± .15	3 61± .24	2 90± .36	4 04± .50	3 90± .76
		5	13	.294±.014	.314±.050	.502± 043	.437± 045		.620±.169	.651± 280	.699± .434
		6	9	.217±.040	.200±.077		.400±.086				
		6	10	1.93± .07	1 03± .21	2 01± .17	2 51± 14		4 45± 52	4.10±1 22	7.21±1 40
		6	11	10 2± .5	11 0± 1 1	21 0± 1 0	18 5± .9		27 0± 2 5	37 0± 3 6	36 9± 5 7
		6	12	32 3± 1 6	22.3± 4 0	60.0± 4 9	65 1± 5 2		91 5±14 4	104 ± 18	126 ± 25
		6	13	19.0± .7	17 0± 1 7	28 6± 1 4	27 7± 1 4	31 9± 2 0	35 8± 3 7	39 9± 5 1	46 9± 8 3
		6	14	2.65± .13	3.64± .38	5 21± .30	4.71± .31	6 29± 46	7 76± 92	7.51±1 30	12 3± 2 2
		6	15	.623± 034	.616± 011	.852± 010	.948± 013		1.13±.079		
		7	12	.333±.020	.397± 049	.658±.055	.731± 071		.916± 179	1.11± 39	
		7	13	4.27± .21	4.49± .46	8.01± .48	8 06± 42		10 7± 1 5	18 6± 2 2	17.0± 3 1
		7	14	29.0± 1.2	31 0± 3 2	49.5± 4 9	41 8± 3 3		72 4±13.6	68 3±23 3	71 2±22 5
		7	15	29.1± 1.9	34 2± 3 3	54.1± 2.7	54.2± 2.9	66 0± 4 3	98 2± 9.6	121.± 15	202 ± 24.
		7	16	.039±.006	.019 ∘	.054±.016	.129±.023	.180±.030		.306±.151	.961 ∘
		8	13	.143±.012	.166±.035	.310±.035	.221±.035		.525±.167		
		8	14	.809±.040	.751±.120	1.60± 10	1.67± .12		2.14± .42	2.20± 58	2.80±1 52
		8	15	23.0± 1.2	27.3± 2.6	43.0± 2.1	42 9± 2 3		74 0± 7 8	99 2±12 6	135.± 22
^{12}C	2.10 GeV/n	1	1 [b]	37 7± 1.9	24.1± 4 1	71 7± 4 2	78 0± 4.2	84.3± 5.7	112.± 9.	131.± 12	171.± 18
		1	2	173.± 9	105.± 19.	329 ± 30	31. ± 28	411 ± 37	543.± 58	690 ± 78	715.±124
		1	3	69.0± 3.4	52 7±10 3	134 ± 10.	129 ± 11	158.± 14	198 ± 24	237.± 32	321 ± 52
		2	3	66.9± 3.3	51.5± 4 5	128 ± 7.	125 ± 7	153 ± 9	192 ± 13	227 ± 16	264 ± 22
		2	4	198.± 10.	171 ± 15	383 ± 39	373.± 33	481.± 48	553.± 59	616 ± 67	728 ± 85
		3	6	1.19± .06	.906± 214	2.54± .25	2.21± .22	2.62± .27	3.21± .47	3.59±1.12	4.21±1.10
		3	8	16.0± .8	13.9± 1.5	33 1± 2 6	30 0± 2 4	36 3± 2 9	47 3± 4 9	56 1± 5 6	66 0± 8 5
		3	7	11.6± .6	11 0± 1 0	22 0± 1 1	21.5± 1 1	27 3± 1 4	31 9± 2 3	40 3± 3 3	45 9± 4 6
		3	8	1.19± .06	1 13± .16	2 52± 16	2.18± .15	2 79± .23	3 89± .47	3.27± 53	3 40± 82
		3	9	.432±.023	.466±.083	.919±.078	.851±.082	.883± 117	1 30± 36	1 20± 33	1 43± 93
		4	7	10.5± .5	9.49± .99	18 5± .9	18 6± 9	25 8± 1 3	33 7± 2.3	41 2± 3 3	47.9± 4 9
		4	9	8.62± .20	5.92±.54	11 0± .5	10 6± 5	12 7± 7	16.1± 1.3	18.6± 1.7	22.5± 2.6
		4	10	3 91± .15	3 42± .35	5 92± .31	5 81± 29	7 02± .40	8.57± 70	8 61± 91	9 97±1 40
		4	11	.089±.004		.018±.008					
		5	8	.756±.038	.468±.110	1.48± .09	1.72± .13	1.76± .19	1.89± .33	1.96± .48	3.69± 76
		5	10	10.5± .5	10 9± 3 9	21.1± 2 6	25 1± 3.9	36 3± 4.8	43.7± 9.8	60.9±17 4	73.0±24 5
		5	11	20 4± 1.4	20 9± 3 4	53.2± 2 9	53 8± 2 7	85 2± 4 7	84 8± 9 8	109 ± 13	155 ± 23
		5	12	.050±.004	.059±.010	.141±.018	.104±.010	.144±.033	.124±.029		110 ∘
		6	9	.257±.017	.370±.074	.936±.056	.539±.066	.697±.086	.924±.172	.920± 264	1.46± 57
		6	10	2 13± .11	2.38± 29	4 20± .21	4.11± .22	4.99± .30	5 38± 95	7.03± 88	7.82±1.07
		6	11	25.5± 1.3	26 1± 2 4	46 7± 2.3	46 5± 2.3	59.9± 3 1	81 3± 6.3	102 ± 10	145 ± 17
		7	12	.035±.004	.031±.010	.058±.011	.079±.011			.048±.096	
^{12}C	1.05 GeV/n	1	1 [b]	10 2± .5	7.03±1 50	20 2± 1.0	18 8± 1.0	24.6± 2 1	26.9± 3 7	35 9± 5 2	46 7± 8 2
		1	2	168 ± 8	125.± 16	301 ± 27	292 ± 26	413 ± 37	489 ± 62	698 ± 82	823 ±149
		1	3	63.6± 3.2		124 ± 7	118 ± 7	149 ± 9.	219.± 19		
		2	3	78 0± 3.9	46 9± 5.1	134 ± 7	135.± 8	161 ± 9.	209 ± 14	237 ± 17	321 ± 26
		2	4	219 ± 11	165.± 19	422.± 30	404 ± 36.	488.± 44.	568 ± 61	727 ± 79	849 ±113
		3	6	.996±.059	.942±.188	2 09± .17	1.83± .19	2.08± .29	3 01± .68	3.61±1.30	7.27±2.67
		3	8	12.5± .6	11 5± 2 2	24 0± 2 0	27.1± 2 2	29.9± 2 9	33.1± 6 8	38 1± 7 6	50 9±13 1
		3	7	11.0± .6	10.9± .8	23.5± 1 2	21 5± 1.1	28 5± 1.9	32.6± 1.9	42 1± 3 6	49 2± 9 0
		3	8	1 18± .06	770±.139	2 36± .19	2.08± .18	2 87± .27	3 99± 78	2.84±1 22	4 94±1 04
		3	9	.399±.026	.399±.093	.755±.078	.673±.096	.810±.159	1.05± 30	1.19± .49	1.76± 81
		4	7	8.93± .45	8 45± 81	17.0± .9	16.6± 9	19.9± 1.1	25.0± 1.5	21 6± 2.7	37 0± 4 7
		4	9	5 71± .29	5 13± 54	11.6± .7	10.7± .5	13.9± .9	19.3± 1.2	23.7± 2.7	22.2± 3 7
		4	10	2.74± .14	3 41± 35	5.68± 30	5.39± .29	6.99± 48	7.69± 61	8.43±1 19	10 9± 1 8
		4	11	.069 ∘		.010±.019					
		5	8	.749±.037	.680±.093	1.55± .08	1.43± .10	1.73± .16	2.29± .32	1.78± .36	2.70± 68
		5	10	10.5± .7	10 2± 2.5	20.0± 2 3	27.9± 2.2	30 9± 3.5	36.9± 9 9	43.1±12.4	58 9±18 2
		5	11	20.9± 1.3	20.3± 2 7	50.7± 3 2	48.6± 2.6	64.5± 5.3	88.1± 7.9	110.± 15	149 ± 25
		5	12	.052±.005	.050±.013	.093±.017	.099±.013	.170±.046	.149±.047		.233 ∘
		6	9	.240±.016	.205±.061	.419±.048	.480±.060	.602±.100	.665±.183	1.19± 30	
		6	10	2 25± 11	2 52± 28	4 82± .23	4 94± .29	5 06± 37	7 93± 78	7.69±1 03	10 9± 1 7
		6	11	20.2± 1.2	23.0± 3 0	44.7± 2 6	44.7± 2 8	57 0± 3.9	78.1± 8.1	98.9±13.3	128 ± 22
		7	12	.019±.005	.053 ∘	.022±.011	.051 ∘	.069±.030			
TARGET FACTOR (Y_T)		1.00		.66+.928A_T	1.99± .02	1.92± .02	2.35± .03	2.81± 06	3.15± 07	3.72± 09	

∘ FACTOR OF 2 ESTIMATE

[b] PROTON PRODUCTION WITHIN 12.5 MR OF 0 DEGREES

Figure Captions

Figure 1. The cross sections for B+T → F + - can be expressed as $\sigma^F_{BT}=\gamma^F_B\gamma_T$, where γ_T is the target factor. Plotted are the mean target factors versus the target mass A_T (amu) for all cross sections given in Table I. The error bars represent the error-weighted standard deviations and reflect the distribution of errors in the individual cross sections σ^F_{BT}. The mean errors for γ_T are approximately the dot size. The computed values of γ_T using the empirical fit are given by the symbol X. Physical parameters in the empirical expression for γ_T are r_T, the half-density charge radius and t, the charge-skin thickness of the target nuclei (see Ref. 13). The line superimposed on the data points is an approximation for $\gamma_T=A_T^{\frac{1}{4}}$.

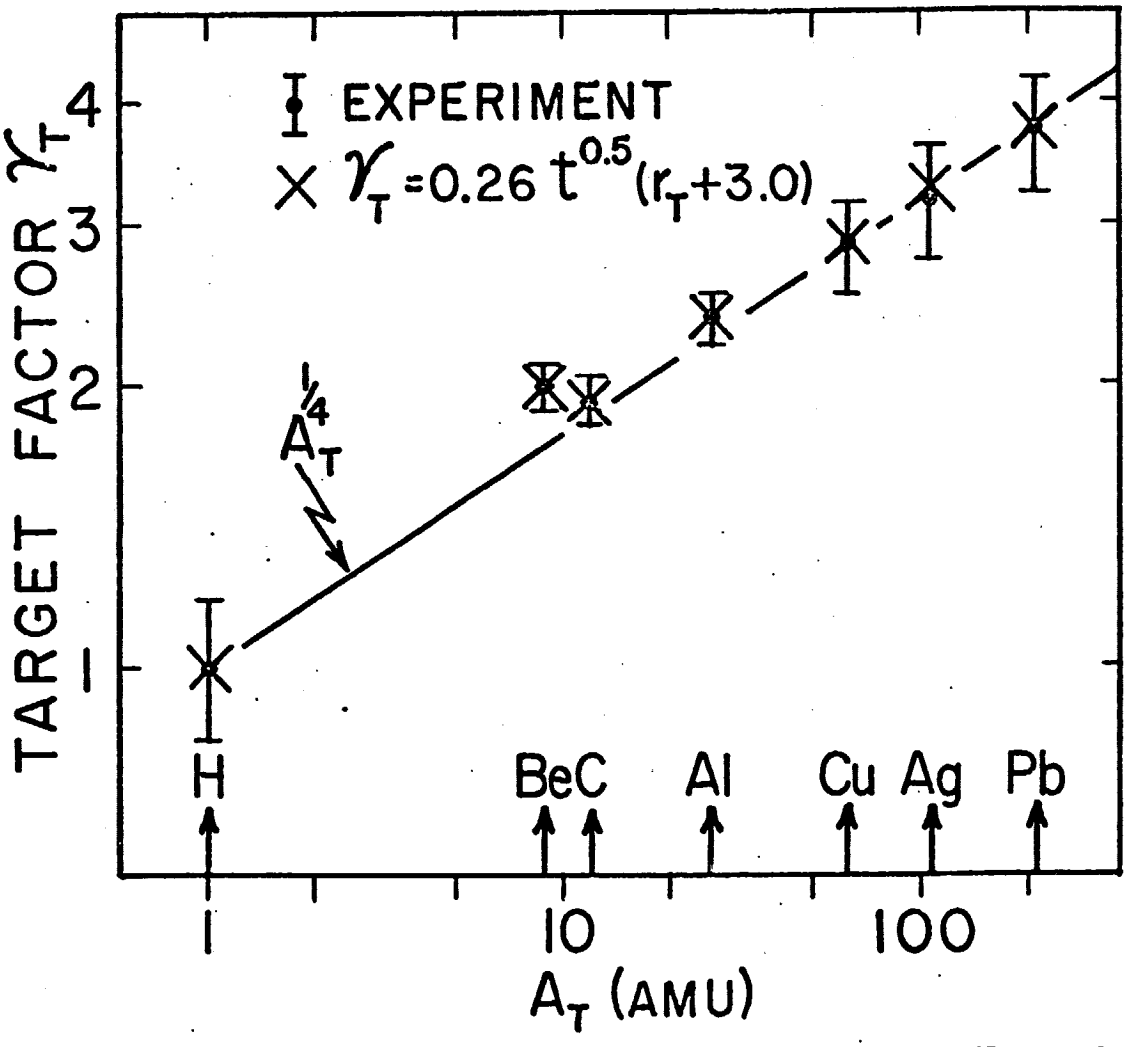
EXPERIMENT
$\gamma_T = 0.26\, t^{0.5}(r_T + 3.0)$
TARGET FACTOR γ_T
$A_T^{1/4}$
H
BeC
Al
Cu
Ag
Pb
1
10
100
A_T (AMU)
XBL 751-130

Fig. 1